MATERIALS SCIENCE

Ferroelectric polarization induces electronic nonlinearity in ion-doped conducting polymers

Simone Fabiano,[1]* Negar Sani,[1]*† Jun Kawahara,[2]‡ Loïg Kergoat,[1]§ Josefin Nissa,[1] Isak Engquist,[1] Xavier Crispin,[1] Magnus Berggren[1]¶

Poly(3,4-ethylenedioxythiophene):polystyrene sulfonate (PEDOT:PSS) is an organic mixed ion-electron conducting polymer. The PEDOT phase transports holes and is redox-active, whereas the PSS phase transports ions. When PEDOT is redox-switched between its semiconducting and conducting state, the electronic and optical properties of its bulk are controlled. Therefore, it is appealing to use this transition in electrochemical devices and to integrate those into large-scale circuits, such as display or memory matrices. Addressability and memory functionality of individual devices, within these matrices, are typically achieved by nonlinear current-voltage characteristics and bistability—functions that can potentially be offered by the semiconductor-conductor transition of redox polymers. However, low conductivity of the semiconducting state and poor bistability, due to self-discharge, make fast operation and memory retention impossible. We report that a ferroelectric polymer layer, coated along the counter electrode, can control the redox state of PEDOT. The polarization switching characteristics of the ferroelectric polymer, which take place as the coercive field is overcome, introduce desired nonlinearity and bistability in devices that maintain PEDOT in its highly conducting and fast-operating regime. Memory functionality and addressability are demonstrated in ferro-electrochromic display pixels and ferro-electrochemical transistors.

INTRODUCTION

Polymer electrochemical devices, particularly those based on poly(3,4-ethylenedioxythiophene):polystyrene sulfonate (PEDOT:PSS), constitute a key family of components that are important for printed electronics (*1*) within existing and emerging applications of smart packaging, textiles (*2*), energy storage (*3*, *4*), medical technology (*5*, *6*), food security (*7*), and transportation (*8*). They are technologically very attractive because they operate at low voltages and are built up from a robust device structure that allows for manufacturing on flexible substrates using low-cost printing techniques. When including polymer electrochemical devices in large-scale electronic systems (*9*, *10*), it is critical that the current-voltage (*I*-*V*) characteristics should be precisely defined. Electronic addressing, memory functionality, and compatibility with specifications of other devices and complete systems can be achieved by introducing well-defined voltage thresholds and nonlinearity in the electrical device performance (*11*).

The terminology "polymer electrochemical devices" is worth a discussion because some of these device concepts deviate from classical electrochemistry (Fig. 1). Electrochemical reactions with inert electrodes are processes that involve electron transfer between the electrode and the reactants in the electrolyte (top electrode of Fig. 1A). If the reactant is immobilized as an insoluble layer in direct contact with the electrode, the reactant is commonly referred to as an electrochemically active solid (bottom electrode in Fig. 1A). Conjugated polymers represent a class of electrochemically active solids that have π-electronic bands, low band gaps, and potentially high ion conductivity that together allow for swift oxidation and reduction of the entire solid bulk in a reversible manner. While reducing or oxidizing a conjugated polymer film, electronic charges provided from the electrode are accumulated or depleted throughout the solid bulk. Those electronic charges are simultaneously compensated by ions that escape from or to the electrolyte (Fig. 1B). Upon changing the redox state of a conjugated polymer, the electronic conductivity, color, and volume are typically controlled. These features serve as the basic mode of operation in a variety of electrochemical devices, such as in the organic electrochemical transistors (OECTs) (*12*, *13*), organic electrochromic displays (OECDs) (*14*, *15*), electro-actuators (*16*), and supercapacitors. PEDOT is currently the most explored conjugated polymer for electrochemical device applications. In its oxidized state, this polymer is commonly charge-compensated by an immobile polymer anion, such as polystyrenesulfonic acid. The resulting PEDOT:PSS polymer blend is highly conductive and can be processed from water emulsions. The PEDOT chains transport holes, whereas the hygroscopic PSS phase provides cation transport (*17*). PEDOT:PSS is therefore referred to as an organic mixed ion-electron conductor (*18*).

In principle, the semiconductor-conductor transition in organic redox polymers offers both nonlinearity and bistability in the current-voltage characteristics, as typically observed in cyclic voltammetry (Fig. 1, A and E) (*19*). The nonlinearity originates from the injection (extraction) of holes (electrons) from the electrode to the valence (conduction) band of the conjugated polymer (*20*). It is tempting to use these electrical features to introduce addressability and bistability of an electrochemical device in passively addressed display or memory matrices. However, the electrical conductivity of the semiconducting state is too low (*21*) and thus limits the speed of the resulting devices, whereas the bistability is poor because of parasitic side reactions (self-discharge phenomenon) (*22*, *23*). Polymer electrochemical devices are commonly made to operate in the fast-switching regime by reducing the operational voltage range such that the neutral semiconducting state is

[1]Laboratory of Organic Electronics, Department of Science and Technology, Linköping University, SE-601 74 Norrköping, Sweden. [2]RISE Acreo, Printed Electronics, Bredgatan 33, Box 787, SE-60117 Norrköping, Sweden.
*These authors contributed equally to this work.
†Present address: RISE Acreo, Printed Electronics, Bredgatan 33, Box 787, SE-60117 Norrköping, Sweden.
‡Present address: Device Materials Laboratory, New Materials Research Department, Research Center, LINTEC Corporation, 7-7-3 Tsuji, Minami-ku, Saitama-shi, Saitama 336-0026, Japan.
§Present address: Institut de Neurosciences des Systèmes, Aix-Marseille University, 13005 Marseille, France.
¶Corresponding author. Email: magnus.berggren@liu.se

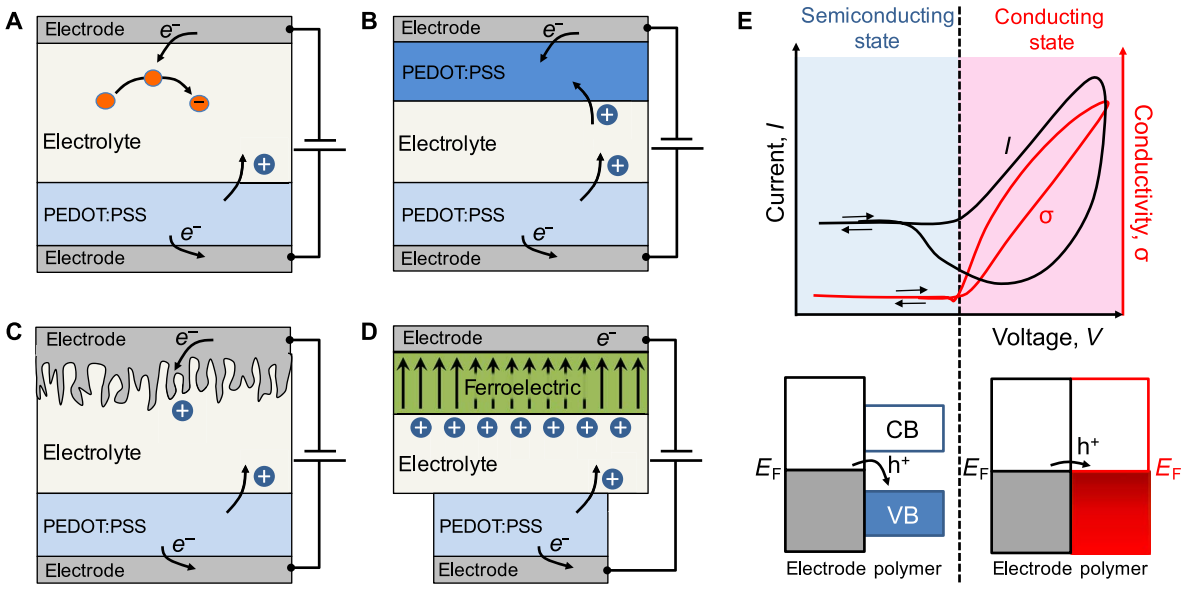

Fig. 1. Operation mode of electrochemical devices. (**A**) Electron transfer between the CE and the reactants in the electrolyte. (**B**) Both the WE and the CE include electrochemically active solids. (**C**) No electron transfer, but charges accumulate at the CE as an EDL, and its capacitance is large enough to fully compensate the charge introduced in the polymer film at the WE. (**D**) The CE consists of a metallic electrode functionalized with a polymer ferroelectric thin-film layer. (**E**) Semiconductor-conductor transition in organic redox polymers showing both nonlinearity and bistability in the *I-V* characteristics, as typically observed in cyclic voltammetry. CB, conduction band; VB, valence band.

never fully reached. The resulting *I-V* characteristics of this device configuration are typically capacitive, thus highly linear in its performance ($I = C \times dV/dt$) and hard to implement and integrate into various circuit applications. The depletion and accumulation of electric charge carriers as well as the exchange of ions upon redox switching of a symmetric PEDOT:PSS two-electrode device cell are illustrated in Fig. 1B.

Reversible operation in asymmetric polymer electrochemical devices traditionally involves redox switching of the conjugated polymer at the working electrode (WE) and a second compensating electrochemical half-reaction at the counter electrode (CE). The half-reaction(s) at the CE is crucial for the resulting switching and *I-V* performance but is, however, often neglected. In particular, it provides us with a tool to introduce nonlinearity and threshold characteristics. When measuring the cyclic voltammetry of the conjugated polymer films, the CE is typically a large-area Pt mesh, where various charge transfer reactions, which ideally do not limit the measured current, occur. Typically, a reference electrode is also used to track the voltage applied on the WE, whereas the voltage on the CE is not considered. However, in an electrochemical device, the WE and CE must be carefully considered to understand what mechanism limits and affects the resulting *I-V* characteristics of the device.

Typically, there are three kinds of mechanisms that can occur at the CE that can potentially dictate the resulting *I-V* characteristics of the electrochemical device: First, charge transfer takes place between the CE and the reactants of the electrolyte (Fig. 1A). Thus, the capacity and electronic energy levels of the CE and the reactants control the evolution of the current running between the WE and the CE. This is, for instance, the case of an acidic aqueous solvent producing dihydrogen at the CE when biased at cathodic potentials (*24*). Second, both the WE and the CE include electrochemically active solids (Fig. 1B). This is, for instance, the case of polymer electrochromic displays, where the active polymer film at one electrode undergoes oxidation and the active polymer film at the other electrode undergoes reduction. The reaction quotient is typically balanced so that the capacity (capacitance) of the CE is equal (symmetric device) or larger than that of the WE to enable full switching of the solid electrochemical material included on the WE. Third, there is no electron transfer, but the charges accumulate along the CE surface as an electric double layer (EDL), and its capacitance is large enough to fully compensate the charge introduced in the polymer film at the WE (Fig. 1C). This is the so-called capacitive displaced electrochemical reaction and has been demonstrated with a neutral (nonoxidized) polymer at the WE and a metallic carbon nanotube network as the CE (*20*) or with a semioxidized polymer included in a small-area WE and driven with a large-area CE (*10*). The net accumulation or depletion of electronic charges within the volume of the polymer film at the WE must here equal the amount of charge stored within the double-layer capacitor residing along the area of the CE. The CE capacitor includes the surface charges accumulated along the CE metal electrode and the inner and outer Helmholtz plane together with the diffuse layer.

Here, we demonstrate yet another CE concept for polymer electrochemical devices, which does not rely on charge transfer but still allows us to introduce desired threshold voltage characteristics and bistability in the resulting *I-V* performance (Fig. 1D) while keeping the conducting polymer in its high conducting state. We explore a CE configuration that consists of a metallic electrode functionalized with a polymer ferroelectric thin-film layer (*25*). In our case, we chose thin films of poly(vinylidenefluoride-*co*-trifluoroethylene) [P(VDF-TrFE)] in contact with a metal electrode. In ferroelectric materials, the spontaneous electric polarization, which can reversibly be switched back and forth as the coercive field is overcome, originates from densely packed and large electric dipoles that are strongly coupled to the polymer material lattice. Ferroelectric polymers have been used in solid-state devices and circuits to introduce addressability and voltage thresholds (*11*, *26*). Because the surface density of dipoles in a ferroelectric material is roughly the same as the density of ions of the inner Helmholtz layer, we are

encouraged to investigate whether a CE coated with a ferroelectric thin film can be used to perform redox switching of the bulk of electrochemical polymer WEs. We apply ferroelectric CEs in electrochromic display cells and circuits and as the gate in electrochemical transistors to introduce desired control in device performance, threshold voltages, and memory functionality.

RESULTS

The molecular structure of PEDOT:PSS is shown in Fig. 1A. In an electrochemical cell, PEDOT:PSS can be switched to its deep blue, semiconducting neutral state, in accordance with the following (Eq. 1)

$$\mathrm{PEDOT^+:PSS^-} + M^+ + e^- \rightleftarrows \mathrm{PEDOT^0} + M^+\mathrm{:PSS^-} \quad (1)$$

where M^+ denotes the positively charged ion and e^- denotes the electron. Hence, the change in electrical conductivity upon electrochemical switching can be exploited in OECTs, whereas the modulation in optical absorption is used in OECDs. Nevertheless, when PEDOT:PSS is used as both the WE and the CE in electrochemical cells (that is, a pixel; Fig. 2B), in contact with a common electrolyte, the degree of ion exchange and charge compensation as well as the pixel coloration occur linearly throughout the whole addressing potential bias window because of the typical capacitive charging behavior of PEDOT:PSS (Fig. 2C). The typical *I-V* characteristics of a pixel are thus governed by the capacitive charging and discharging of the electrodes with a consequent lack of any threshold, bistability, or rectification behavior that would allow for passive matrix addressing or memory functionality (Fig. 2C). The typical bulk charge density of the PEDOT:PSS film with a thickness of d = 100 to 200 nm is about 100 to 300 μC cm^{-2}, which corresponds to a total amount of stored bulk charges Q_{PEDOT} of about 0.3 to 0.8 μC, considering a pixel area of 0.0025 cm^2 (Fig. 2D).

The ferroelectric fluorinated polymer P(VDF-TrFE) (Fig. 3A) can maintain an electric polarization state in the absence of an externally applied electric field. The polarization state and the resulting surface charge density originate from a bistable, switchable dipole moment, maintained across the ferroelectric crystalline domains of the material (fig. S1). Figure 3A shows the typical *I-V* characteristic for a capacitor with a 140-nm-thick P(VDF-TrFE) ferroelectric layer. The current peaks located at around ±10 V are due to the ferroelectric polarization (coercive field of about 70 MV m^{-1}). The net ferroelectric surface charge (Q_{PVDF}) can be induced to be either positive or negative depending on the direction of the applied polarizing electric field. Dielectric displacement measurements performed at 100-Hz yield a remnant surface charge, normalized to the device surface area, of about 8 to 10 μC cm^{-2} (Fig. 3B).

When a ferroelectric P(VDF-TrFE) thin film deposited onto a bottom metal substrate is used as CE in an OECD structure, a rather different behavior of the PEDOT pixel *I-V* characteristics is observed (Fig. 4). At positive voltage bias, where the pixel switches from the conducting light blue–colored state to the semiconducting dark blue–colored state, a fairly small current is observed until the applied potential reaches the coercive voltage, defined as the minimum voltage bias required to fully switch the remanent ferroelectric polarization of dipoles. Because of the high ferroelectric surface charge density, which is typically on the order of 8 to 10 μC cm^{-2} for P(VDF-TrFE) films (see above), an EDL is established at the ferroelectric/electrolyte interface, whereas the ferroelectric polarization charge is compensated by free charges at the bottom metal electrode. The polarization switching time is not limited or affected by the polyelectrolyte interlayer (*27*). Furthermore, recent studies have shown that dipolar interactions identified as Coulomb attractions between hydrogen atoms in the PVDF chains and anions promote switching of ferroelectric polarization (*28*). In this respect, polyelectrolytes, ionic liquids, and polymer electrolytes containing various kinds of electrolyte components can supply enough of

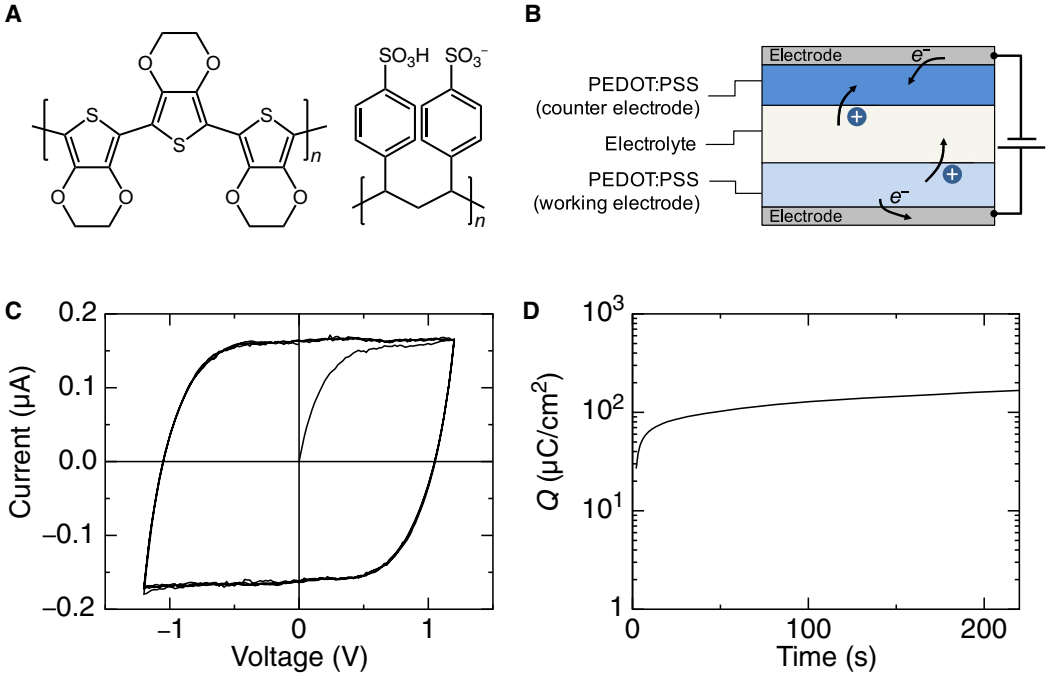

Fig. 2. Electrical characteristics of PEDOT:PSS. (**A**) Chemical structure of PEDOT:PSS. (**B**) Schematic of a symmetric PEDOT:PSS/electrolyte/PEDOT:PSS. (**C**) Typical *I-V* characteristics of a device at 0.4 V s^{-1}. (**D**) Reduction of pristine PEDOT:PSS electrodes at −0.8 V.

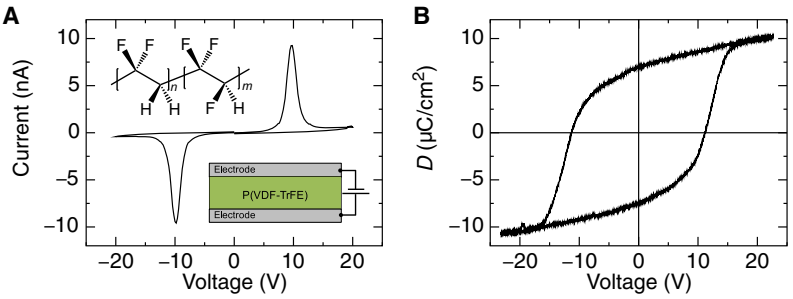

Fig. 3. Electrical characteristics of P(VDF-TrFE). (**A**) Typical *I-V* characteristics of a Au/P(VDF-TrFE)/Au device. The inset shows the chemical structure of P(VDF-TrFE) and the device structure. (**B**) Ferroelectric hysteresis loops of a 140-nm-thick layer using a Sawyer-Tower circuit at a 100-Hz applied voltage frequency.

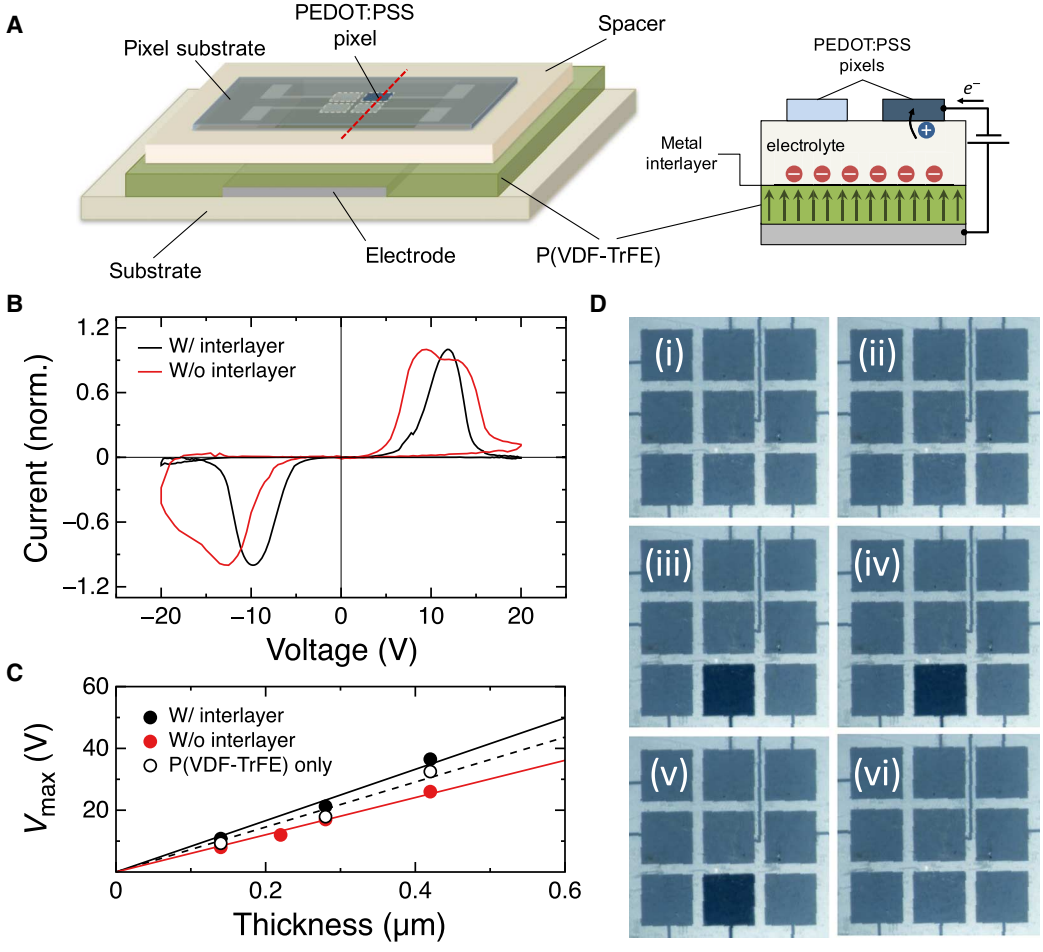

Fig. 4. Electrical characteristics of a ferroelectric PEDOT:PSS pixel. (**A**) Schematic of the ferroelectric PEDOT:PSS pixel and its cross section. (**B**) Normalized *I-V* characteristics of a typical ferro-electrochemical pixel with (black curve) and without (red curve) metal interlayer. (**C**) Peak voltage as a function of P(VDF-TrFE) film thickness for ferro-electrochemical pixel with (black dots) and without (red dots) metal interlayer. Open dots refer to a metal/P(VDF-TrFE)/metal capacitor. (**D**) Optical images of a printed passive matrix–addressed electrochromic display containing 3 × 3 ferro-electrochemical pixels with metal interlayer. Indices (i to vi) are displayed in fig. S4 for clarity.

the charges needed for a full compensation of the sheet of ferroelectric dipoles to stabilize the domains during the switching process. Because the typical bulk charge density of a 100-nm-thick PEDOT:PSS film is about 100 to 150 μC cm^{-2} (that is, total bulk charge Q_{PEDOT} of 0.3 to 0.4 μC, considering a pixel area of 0.0025 cm^2), a Q_{PEDOT}/Q_{PVDF} charge ratio of 1:1 or smaller is thus required to fully switch the PEDOT:PSS bulk in between the different electronic states given by Eq. 1. When the ferroelectric polymer is poled by a positive bias voltage applied to the bottom electrode causing the dipoles to flip, a displacement current is established through the ferroelectric layer, resulting in a rapid increase of the current level. PEDOT^{m+} then starts to be chemically reduced to PEDOT^{n+} (dark blue state and $m > n$). The reduction of PEDOT^{m+} continues with an increasing current until most, but not all, of the chain segments turn neutral (PEDOT^0). The process saturates at

a voltage of around 11 to 12 V, which corresponds to the expected coercive voltage for a ferroelectric layer thickness of about 140 nm. At even higher positive voltages, a permanent decrease in film conductivity is observed; thus, PEDOT is now in its nonconducting neutral and semiconducting state. The dark blue–colored state of PEDOT$^{m+/0}$ is maintained until the ferroelectric dipoles are switched back in the opposite direction upon application of a negative potential to the bottom electrode (Fig. 4B). To avoid overoxidizing the PEDOT electrode pixel, it is important that the voltage bias is not swept beyond the actual switch voltage of the device, that is, beyond −20 V. We note that, although the maximum current occurs at a bias that corresponds to the expected coercive field, the current offset appears at a voltage bias lower than the one expected for the specific ferroelectric thickness. This may be the result of a non-negligible dielectric displacement current of the insulator that is high enough to reduce PEDOT^{m+}. Although P(VDF-TrFE) films are morphologically smooth after spin coating, thermal annealing causes crystal growth that increases the surface roughness (*29*). The shift of the offsets toward a lower voltage might thus be due to slow diffusion of ions into these morphologically distinct voids, which alters the ferroelectric film morphology, leading to a high leakage current and device failure upon multiple cycles (fig. S2). Recently developed methodologies for the fabrication of smoother PVDF films (*30*) may improve the reliability of ferroelectric devices in aqueous and electrolytic environments. To avoid or reduce this leakage, we included here a metal interlayer in between the P(VDF-TrFE) film and the electrolyte. This metal interlayer does not affect the properties of the ferroelectric film, nor the resulting device performance, but it protects the ferroelectric from any influx of ions (fig. S3). Figure 4B shows the *I-V* characteristics of the PEDOT:PSS pixel comprising the metal interlayer. The voltage required to switch the ferroelectric polarization can be controlled, without any loss of the ferroelectric surface charge density, by increasing/decreasing the ferroelectric layer thickness. Figure 4C shows the current peak voltage values as a function of the P(VDF-TrFE) film thickness. A linear correlation is found regardless of the inclusion of the metal interlayer, with voltage levels similar to those found in P(VDF-TrFE) capacitor devices (open symbols). Insertion of the metal interlayer between the P(VDF-TrFE) layer and the electrolyte prevents ion penetration and thus device failure upon multiple cycles (fig. S3). Figure 4D shows a printed passive matrix–addressed electrochromic display containing 3 × 3 ferroelectrochemical pixels (movie S1). The well-defined ferroelectric polarization results in a desired *I-V* threshold (fig. S4) that enables simple addressability without cross-talk, which promises for high-volume and low-cost production of flexible displays. The color of the PEDOT:PSS can be controlled by changing the area of the ferroelectric-electrolyte interface (that is, Q_{PVDF}; fig. S5). This is qualitatively similar to controlling the amount of charge injected into the PEDOT layer of a symmetric PEDOT:PSS/electrolyte/PEDOT:PSS pixel by means of an applied voltage bias (*31*).

The hysteretic switching of the electronic states of PEDOT, achieved using a ferroelectric polymer CE, is also reflected in a threshold switching of the resistive state. The modulation of the in-plane conductivity is preferably characterized by means of a three-terminal device, that is, the OECT (*32*). The operation of a PEDOT-based OECT relies on the reversible ion exchange and charge compensation switching of the PEDOT:PSS channel that modulates the electronic conductivity between the source and the drain contact. This doping and dedoping of PEDOT can result in conductivity changes of several orders of magnitude with consequent modulation of drain-source current (I_d). Figure 5 demonstrates an OECT, where the conducting PEDOT:PSS polymer system was printed on a flexible plastic substrate. In typical PEDOT-based OECTs, the drain current decreases with gate voltage (V_g), consistent with the operation of a p-type depletion-mode transistor (see Fig. 5A). When a positive bias is applied at the gate, cations from the electrolyte enter the PEDOT:PSS film and compensate the pendant sulfonate anions along the PSS polyanion. This leads to a decrease of the hole density within the PEDOT phase, because holes extracted at the drain are not reinjected by the source terminal. This then results in a decrease of the drain current, with an associated transconductance defined as $g = dI_d/dV_g$ reaching a maximum of about 0.3 mS at V_g ranging from 0.25 to 0.6 V (Fig. 5B). When the ferroelectric layer is included in the gate configuration, the displacement current of the ferroelectric layer, provided from switching of ferroelectric dipoles, dictates the gate current of the resulting OECT. Therefore, the thickness of the ferroelectric layer determines the coercive voltage and, consequently, the modulation of the current of the channel. Upon varying the gate voltage, the conductivity of the channel is constant until the coercive field of the ferroelectric material is reached (see Fig. 5C). As soon as the coercive voltage is overcome, the dipole displacement current of the ferroelectric flows through the gate. This decreases (high resistive state, low current) or increases (low resistive state, high current) the number of charge carriers of the PEDOT channel. The accompanying current switching is observed as sharp features in the gate current at ±14 to 18 V [the P(VDF-TrFE) film thickness is ca. 280 nm], and as steep increase and decrease of the drain current, depending on the switching direction of the ferroelectric dipoles. Note that the on/off current ratio is dictated by Q_{PVDF} (fig. S6), as also shown above for the coloring of the pixel. The characteristic performance of the OECT, which includes the ferroelectric layer gate configuration, confirms that the memory effect is driven by ferroelectric polarization switching, rather than any charge trapping mechanisms or ion migration in and through the ferroelectric layer. Hence, the transistor behaves as a bistable and addressable memory cell element. Accordingly, the transconductance peaks just at V_g bias levels, where the ferroelectric layer is being poled, whereas it is negligible at the V_g kept below the coercive field of the ferroelectric layer (see Fig. 5D). Here, the transconductance value has been normalized considering the drop of potential over the P(VDF-TrFE) layer. The advantage of our ferroelectric OECTs compared to previously reported organic ferroelectric field-effect transistors (FeFETs) (*33*, *34*) is that ions in the former interact with the whole volume of the active material, giving rise to lower impedance and higher transconductance.

We also investigated the transient response and retention time of the printed ferroelectric OECTs (figs. S7 and S8). The use of P(VDF-TrFE)–coated gate electrode does not affect the on-to-off state transition of the printed OECTs, which is found to be as fast as ~0.02 s. Note that this value is comparable to the on-to-off switching time of our printed PEDOT:PSS-based OECTs having PEDOT:PSS as the gate electrode (see fig. S7). On the other hand, the off-to-on state transition is found to occur within seconds, indicating that the programming time is primarily determined by the conductance of the conductor channel, as also observed for unipolar FeFETs (*33*). The retention time of the ferroelectric OECT's on/off states was investigated by measuring the remnant drain current level as a function of time (fig. S8). Long retention time is distinctive of ferroelectric capacitors and organic FeFETs (*33*). When PEDOT:PSS is in its high conductive state (on state), the current does not change with time because of the high air stability of the oxidized PEDOT. However, when PEDOT:PSS

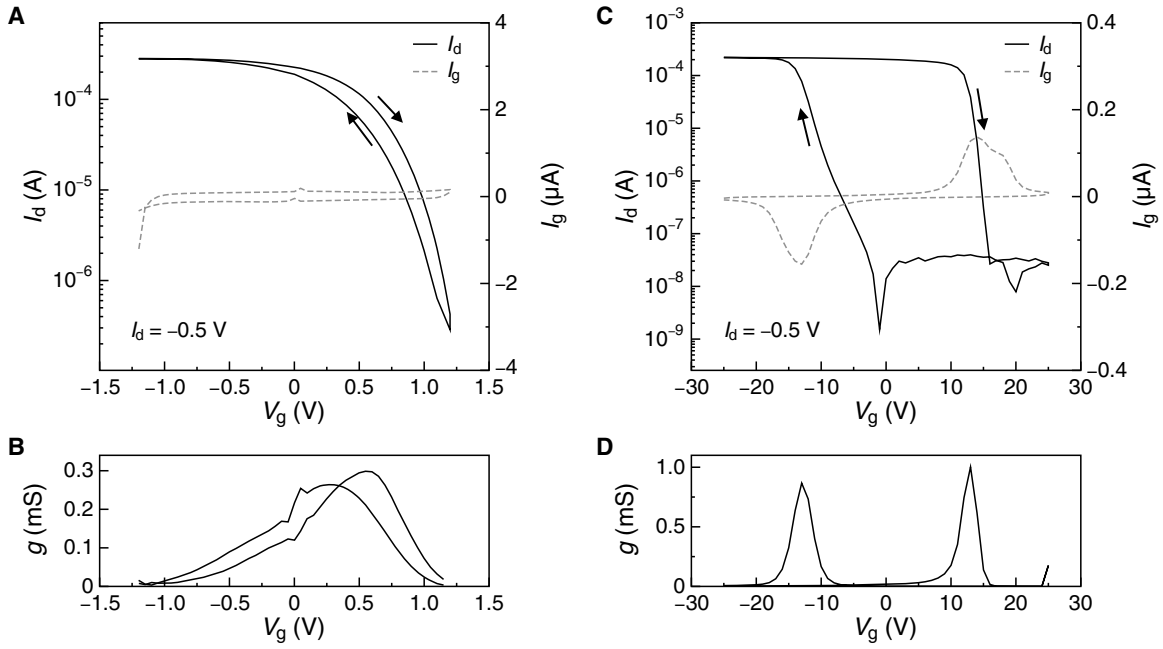

Fig. 5. Steady-state characteristics of electrochemical transistors. Transfer characteristics of an ECT with 100-μm-long PEDOT:PSS channel (V_d = −0.5 V) (**A**) and the associated transconductance (**B**). Transfer characteristics of a ferroelectric ECT with 100-μm-long PEDOT:PSS channel and 280-nm-thick P(VDF-TrFE) dielectric (V_d = −0.5 V) (**C**) and the associated transconductance (**D**).

is in its neutral (reduced) off state, it undergoes oxygen doping upon exposure to ambient atmosphere because of its strong electron-donor character. This results in a gradual increase of the electrical conductivity with time, which hampers long retention. This vulnerability of the reduced PEDOT:PSS to oxidation under ambient conditions can typically be precluded by operating the devices under inert conditions (for example, encapsulation).

DISCUSSION

Polymer electrochemical devices, in particular those based on PEDOT, have been extensively explored during the past two decades in existing and emerging applications. Used as the WE, PEDOT exhibits typical linear and capacitive current versus voltage characteristics. This device performance cannot directly be used to achieve memory or address functionality, which is needed for further integration of the devices to form circuits. With well over 2000 manuscripts reporting PEDOT-based electrochemical devices, very little efforts have been devoted to make these devices addressable and to have the necessary bistability characteristics. We demonstrate that ferroelectric polymers such as P(VDF-TrFE) combined with metals used as the CE can be used to introduce desired threshold voltage characteristics and bistability in the *I-V* performance of the redox polymers while maintaining the latter in their high conducting state. We include this ferroelectric CE configuration in OECDs and as the gate electrode in OECTs. In OECDs, the ferroelectric CE introduces a clear threshold voltage and desired bistability, thus allowing us to realize passively addressed display matrices. In OECTs, the ferroelectric CE makes the transconductance peak at two distinctly different gate voltages, depending on the polarization of the ferroelectric film, thus making the OECT become an addressable memory element. The concept of combining redox polymers with ferroelectric-based electrodes is also potentially very interesting for many other components and circuits. We imagine that this ferro-electrochemical device concept can also be applied to, for instance, sensors, charge storage systems, logics, multiplexers, shift registers, and more.

MATERIALS AND METHODS

Fabrication of P(VDF-TrFE) films

The ferroelectric P(VDF-TrFE) 70/30 mol % copolymer, purchased from Solvay SA, was dissolved in diethyl carbonate at a concentration of 4 wt % and filtered through a 0.45-μm filter. A gold bottom electrode was deposited on a Si substrate via thermal evaporation. The prepared P(VDF-TrFE) solution was spin-coated on the bottom electrode with a 2000-rpm spin rate for 30 s and annealed in air at 130°C for 20 min to obtain a 140-nm-thick film. To deposit thicker films, the spin-coating step was repeated a number of times (according to the desired thickness). For the devices with the interlayer, an aluminum top electrode is also deposited via thermal evaporation.

Preparation of PEDOT:PSS pixels

A plastic foil of polyethylene terephthalate (PET) wet-coated with a thin PEDOT:PSS layer on top was used as a substrate (AGFA-Gevaert Orgacon F-350). The substrate was rinsed in acetone, deionized water, and isopropanol and baked at 110°C for 10 min. Shipley S1805 photoresist was then spin-coated onto the surface. The substrate was exposed with a mask aligner (Suss MA/BA6) and developed in Microposit MF-319. After a baking step at 110°C for 10 min, the pattern was dry-etched using O_2/CF_4 plasma. The remaining photoresist was removed with Shipley 1112A, and the substrate was rinsed in acetone and deionized water. The pixel size was 500 × 500 μm^2. The electrolyte Luviquat (purchased from BASF) was placed on top of the prepared P(VDF-TrFE) film, and the patterned PEDOT:PSS pixels were laminated on the electrolyte and pressed to obtain a thickness of a few millimeters. TiO_2 particles were added to Luviquat to make the electrolyte sufficiently

opaque and thus to increase the contrast of the display in Fig. 4D. In the devices with the interlayer, a layer of aluminum was deposited by thermal evaporation on top of the P(VDF-TrFE) film before the electrolyte was applied.

Preparation of electrochemical transistors

Source, drain, and channel active material of the transistors were screen-printed on PET plastic foils. The source and drain electrodes consist of a carbon conductive composition (DuPont 7102). The channel (100 μm in length and 375 μm in width), which connects the source to the drain, was made of PEDOT:PSS. An insulator layer was screen-printed on top of the source, drain, and PEDOT:PSS channel. An opening in the insulator permits the gate to come in contact with the channel through an electrolyte. Bistability was induced in the OECT by connecting the gate of the transistor to a P(VDF-TrFE) capacitor. The top aluminum layer was deposited on top of the prepared P(VDF-TrFE) film to obtain a P(VDF-TrFE) capacitor. The capacitor was connected to the gate of the OECT via external wiring or by lamination.

Materials and device characterization

Atomic force microscopy (Dimension Icon) was performed in tapping mode using a silicon cantilever having a spring constant of 40 N/m.

The charge displacement measurements were performed using a Sawyer-Tower circuit with an Agilent function generator connected to the input and the oscilloscope recording the output. The other electrical characteristics of the devices are measured using a semiconductor parameter analyzer (Keithley 4200-SCS).

For recording the electrochromism of the PEDOT:PSS pixels, a video was captured using a Nikon SMZ1500 via a microscope while the input voltage was applied to the pixels by the parameter analyzer. The images were extracted from the video and enhanced using a MATLAB code to clarify the contrast between the on and off pixels.

SUPPLEMENTARY MATERIALS

Supplementary material for this article is available at http://advances.sciencemag.org/cgi/content/full/3/6/e1700345/DC1

fig. S1. Morphology characterization of P(VDF-TrFE) films.
fig. S2. Morphology characterization and stability test of P(VDF-TrFE) without metal interlayer.
fig. S3. Morphology characterization and stability test of P(VDF-TrFE) with metal interlayer.
fig. S4. *I-V* characteristic of the ferro-electrochemical pixel reported in Fig. 4D.
fig. S5. Optical images of printed electrochromic displays and grayscale pixel intensity distribution analysis.
fig. S6. Transfer characteristics of a ferroelectric OECT with Q_{PVDF} 2/3 of Q_{PEDOT}.
fig. S7. Transient response of ferroelectric PEDOT:PSS-based OECTs.
fig. S8. Data retention time of ferroelectric PEDOT:PSS-based OECTs.
movie S1. Printed passive matrix–addressed electrochromic displays.

REFERENCES AND NOTES

1. M. Berggren, D. Nilsson, N. D. Robinson, Organic materials for printed electronics. *Nat. Mater.* **6**, 3–5 (2007).
2. H. K. Kim, M. S. Kim, S. Y. Chun, Y. H. Park, B. S. Jeon, J. Y. Lee, Y. K. Hong, J. Joo, S. H. Kim, Characteristics of electrically conducting polymer-coated textiles. *Mol. Cryst. Liquid Cryst.* **405**, 161–169 (2003).
3. Y. Kudoh, K. Akami, Y. Matsuya, Solid electrolytic capacitor with highly stable conducting polymer as a counter electrode. *Synth. Met.* **102**, 973–974 (1999).
4. S. Ghosh, O. Inganäs, Nano-structured conducting polymer network based on PEDOT-PSS. *Synth. Met.* **121**, 1321–1322 (2001).
5. D. Khodagholy, T. Doublet, P. Quilichini, M. Gurfinkel, P. Leleux, A. Ghestem, E. Ismailova, T. Hervé, S. Sanaur, C. Bernard, G. G. Malliaras, In vivo recordings of brain activity using organic transistors. *Nat. Commun.* **4**, 1575 (2013).
6. D. Khodagholy, J. N. Gelinas, Z. Zhao, M. Yeh, M. Long, J. D. Greenlee, W. Doyle, O. Devinsky, G. Buzsáki, Organic electronics for high-resolution electrocorticography of the human brain. *Sci. Adv.* **2**, e1601027 (2016).
7. Z. Wang, H. Zhang, Z. Wang, J. Zhang, X. Duan, J. Xu, Y. Wen, Trace analysis of Ponceau 4R in soft drinks using differential pulse stripping voltammetry at SWCNTs composite electrodes based on PEDOT:PSS derivatives. *Food Chem.* **180**, 186–193 (2015).
8. M. Nikolou, G. G. Malliaras, Applications of poly(3,4-ethylenedioxythiophene) doped with poly(styrene sulfonic acid) transistors in chemical and biological sensors. *Chem. Rec.* **8**, 13–22 (2008).
9. P. Andersson, D. Nilsson, P.-O. Svensson, M. Chen, A. Malmström, T. Remonen, T. Kugler, M. Berggren, Active matrix displays based on all-organic electrochemical smart pixels printed on paper. *Adv. Mater.* **14**, 1460–1464 (2002).
10. J. Rivnay, P. Leleux, M. Sessolo, D. Khodagholy, T. Hervé, M. Fiocchi, G. G. Malliaras, Organic electrochemical transistors with maximum transconductance at zero gate bias. *Adv. Mater.* **25**, 7010–7014 (2013).
11. K. Asadi, P. W. M. Blom, D. M. de Leeuw, The MEMOLED: Active addressing with passive driving. *Adv. Mater.* **23**, 865–868 (2011).
12. S. Chao, M. S. Wrighton, Characterization of a solid-state polyaniline-based transistor: Water vapor dependent characteristics of a device employing a poly(vinyl alcohol)/phosphoric acid solid-state electrolyte. *J. Am. Chem. Soc.* **109**, 6627–6631 (1987).
13. D. Nilsson, M. Chen, T. Kugler, T. Remonen, M. Armgarth, M. Berggren, Bi-stable and dynamic current modulation in electrochemical organic transistors. *Adv. Mater.* **14**, 51–54 (2002).
14. A. A. Argun, P.-H. Aubert, B. C. Thompson, I. Schwendeman, C. L. Gaupp, J. Hwang, N. J. Pinto, D. B. Tanner, A. G. MacDiarmid, J. R. Reynolds, Multicolored electrochromism in polymers: Structures and devices. *Chem. Mater.* **16**, 4401–4412 (2004).
15. Q. Pei, G. Zuccarello, M. Ahlskog, O. Inganäs, Electrochromic and highly stable poly(3,4-ethylenedioxythiophene) switches between opaque blue-black and transparent sky blue. *Polymer* **35**, 1347–1351 (1994).
16. Q. Pei, O. Inganäs, Electrochemical muscles: Bending strips built from conjugated polymers. *Synth. Met.* **57**, 3718–3723 (1993).
17. J. Rivnay, S. Inal, B. A. Collins, M. Sessolo, E. Stavrinidou, X. Strakosas, C. Tassone, D. M. Delongchamp, G. G. Malliaras, Structural control of mixed ionic and electronic transport in conducting polymers. *Nat. Commun.* **7**, 11287 (2016).
18. C. M. Proctor, J. Rivnay, G. G. Malliaras, Understanding volumetric capacitance in conducting polymers. *J. Polym. Sci. B Polym. Phys.* **54**, 1433–1436 (2016).
19. M. C. Morvant, J. R. Reynolds, In situ conductivity studies of poly(3,4-ethylenedioxythiophene). *Synth. Met.* **92**, 57–61 (1998).
20. O. Larsson, A. Laiho, W. Schmickler, M. Berggren, X. Crispin, Controlling the dimensionality of charge transport in an organic electrochemical transistor by capacitive coupling. *Adv. Mater.* **23**, 4764–4769 (2011).
21. M. Erginer, E. Sezer, B. Ustamehmetoğlu, J. Heinze, Voltammetric, electrochemical quartz crystal microbalance and in situ conductance studies of conducting polymers based on ethylenedioxythiophene and N-ethylcarbazole. *Electrochim. Acta* **67**, 181–186 (2012).
22. K. Shinozaki, A. Kabumoto, H. Sato, Mechanism of self-discharge in conductive polymer electrodes. *Synth. Met.* **38**, 135–141 (1990).
23. H. Olsson, E. J. Berg, M. Strømme, M. Sjödin, Self-discharge in positively charged polypyrrole–cellulose composite electrodes. *Electrochem. Commun.* **50**, 43–46 (2015).
24. P. Andersson Ersman, J. Kawahara, M. Berggren, Printed passive matrix addressed electrochromic displays. *Org. Electron.* **14**, 3371–3378 (2013).
25. D. Zhao, I. Katsouras, M. Li, K. Asadi, J. Tsurumi, G. Glasser, J. Takeya, P. W. M. Blom, D. M. de Leeuw, Polarization fatigue of organic ferroelectric capacitors. *Sci. Rep.* **4**, 5075 (2014).
26. K. Asadi, J. Wildeman, P. W. M. Blom, D. M. De Leeuw, Retention time and depolarization in organic nonvolatile memories based on ferroelectric semiconductor phase-separated blends. *IEEE Trans. Electron Dev.* **57**, 3466–3471 (2010).
27. S. Fabiano, X. Crispin, M. Berggren, Ferroelectric polarization induces electric double layer bistability in electrolyte-gated field-effect transistors. *ACS Appl. Mater. Interfaces* **6**, 438–442 (2014).
28. F. Wang, A. Lack, Z. Xie, P. Frübing, A. Taubert, R. Gerhard, Ionic-liquid-induced ferroelectric polarization in poly(vinylidene fluoride) thin films. *Appl. Phys. Lett.* **100**, 062903 (2012).
29. S. Fabiano, H. Usta, R. Forchheimer, X. Crispin, A. Facchetti, M. Berggren, Selective remanent ambipolar charge transport in polymeric field-effect transistors for high-performance logic circuits fabricated in ambient. *Adv. Mater.* **26**, 7438–7443 (2014).
30. M. Li, H. J. Wondergem, M.-J. Spijkman, K. Asadi, I. Katsouras, P. W. M. Blom, D. M. de Leeuw, Revisiting the δ-phase of poly(vinylidene fluoride) for solution-processed ferroelectric thin films. *Nat. Mater.* **12**, 433–438 (2013).
31. J. Kawahara, P. A. Ersman, I. Engquist, M. Berggren, Improving the color switch contrast in PEDOT:PSS-based electrochromic displays. *Org. Electron.* **13**, 469–474 (2012).

32. D. Khodagholy, J. Rivnay, M. Sessolo, M. Gurfinkel, P. Leleux, L. H. Jimison, E. Stavrinidou, T. Herve, S. Sanaur, R. M. Owens, G. G. Malliaras, High transconductance organic electrochemical transistors. *Nat. Commun.* **4**, 2133 (2013).
33. R. C. G. Naber, C. Tanase, P. W. M. Blom, G. H. Gelinck, A. W. Marsman, F. J. Touwslager, S. Setayesh, D. M. de Leeuw, High-performance solution-processed polymer ferroelectric field-effect transistors. *Nat. Mater.* **4**, 243–248 (2005).
34. R. Schroeder, L. A. Majewski, M. Grell, All-organic permanent memory transistor using an amorphous, spin-cast ferroelectric-like gate insulator. *Adv. Mater.* **16**, 633–636 (2004).

Acknowledgments: We thank P. Andersson Ersman and X. Wang (Acreo) for providing the printed OECTs and useful discussion. **Funding:** This research was partially supported by the Advanced Functional Materials Center at Linköping University and the Önnesjö Foundation. The authors thank the Knut and Alice Wallenberg Foundation (Power Paper project, scholars) and the Swedish Foundation for Strategic Research (Synergy project) for financial support. S.F. gratefully acknowledges funding by the Swedish Governmental Agency for Innovation Systems (VINNOVA) (grant no. 2015-04859) and the Swedish Research Council (grant no. 2016-03979). **Author contributions:** S.F., X.C., and M.B. conceived and designed the project. S.F. and J.K. initiated the study. N.S. fabricated the devices and performed the electrical measurements. L.K. performed photolithography. S.F. and N.S. analyzed the data. S.F., N.S., X.C., and M.B. wrote the paper. All authors revised and approved the manuscript. **Competing interests:** S.F., N.S., J.K., X.C., and M.B. filed a patent related to this work, through the European Patent Office (application no. EP16163523, filed 1 April 2016). The other authors declare that they have no competing interests. **Data and materials availability:** All data needed to evaluate the conclusions in the paper are present in the paper and/or the Supplementary Materials. Additional data related to this paper may be requested from the authors.

Submitted 1 February 2017
Accepted 11 May 2017
Published 30 June 2017
10.1126/sciadv.1700345

Citation: S. Fabiano, N. Sani, J. Kawahara, L. Kergoat, J. Nissa, I. Engquist, X. Crispin, M. Berggren, Ferroelectric polarization induces electronic nonlinearity in ion-doped conducting polymers. *Sci. Adv.* **3**, e1700345 (2017).

Ferroelectric polarization induces electronic nonlinearity in ion-doped conducting polymers

Simone Fabiano, Negar Sani, Jun Kawahara, Loïg Kergoat, Josefin Nissa, Isak Engquist, Xavier Crispin and Magnus Berggren

Sci Adv **3** (6), e1700345.
DOI: 10.1126/sciadv.1700345